First step to the improvement of the blood brain barrier passage of atazanavir encapsulated in sustainable bioorganic vesicles

Florian Nolay, Emmanuel Sevin, Mathieu Létévé, Abed Bil, Fabien Gosselet, Karim El Kirat, Florence Djedaini-Pilard, Sandrine Morandat, Laurence Fenart, Cédric Przybylski, et al.

Version of Record: https://www.sciencedirect.com/science/article/pii/S0378517320305883
Manuscript_4051ab82c768a9de82c50bc6b249b231

First step to the improvement of the blood brain barrier passage of atazanavir encapsulated in sustainable bioorganic vesicles.

Florian Nolay,[1] Emmanuel Sevin,[2] Mathieu Létévé,[1] Abed Bil,[1] Fabien Gosselet,[2] Karim El Kirat,[3] Florence Djedaini-Pilard,[1] Sandrine Morandat,[4] Laurence Fenart,[2] Cédric Przybylski,[5] Véronique Bonnet[1]*

1 LG2A UMR CNRS 7378 Institut de Chimie de Picardie FR CNRS 3085, SFR Condorcet, Université de Picardie Jules Verne, 33 rue St Leu 80039 Amiens France, veronique.bonnet@u-picardie.fr
2 Univ. Artois, UR2465, BBB Laboratory, 62300 Lens, France
3 BMBI UMR CNRS 7338 Centre de Recherche Royallieu, Université de Technologie de Compiègne, 60203 Compiègne, France
4 GEC FRE CNRS 3580 Centre de Recherche Royallieu, Université de Technologie de Compiègne, 60203 Compiègne, France
5 Sorbonne Université, CNRS, Institut Parisien de Chimie Moléculaire, IPCM, 4 Place Jussieu, 75005 Paris, France

Abstract:
The blood brain barrier (BBB) prevents the majority of therapeutic drugs from reaching the brain following intravenous or oral administration. In this context, polymer nanoparticles are a promising alternative to bypass the BBB and carry drugs to brain cells. Amphiphilic cyclodextrins can form self-assemblies whose nanoparticles have a 100-nm-diameter range and are thus able to encapsulate drugs for controlled release. Our goal is to propose an optimized chemical synthesis of amphiphilic cyclodextrin, which remains a challenging task which commonly leads to only a low-milligram level of the high purity compound. Such cyclodextrin derivatives were used to prepare vesicles and to study their ability to vectorize a drug through the BBB. As a result, we introduced a convergent synthesis for a family of lipophosphoramidyl permethylated β-CDs (Lip-β-CDs) with various chain lengths. It was demonstrated that mixed vesicles comprised of phosphatidylcholine (POPC) and LipCDs were able to encapsulate atazanavir (ATV), a well-known protease inhibitor used as an antiretroviral drug against HIV. We highlighted that neo-vesicles promote the penetration of ATV in endothelial cells of the BBB, presumably due to the low fusogenicity of Lip-β-CDs.

Keywords: Amphiphilic Cyclodextrin, vesicles, Vectorisation, Atazanavir, Blood Brain Barrier

1. Introduction

The blood−brain barrier (BBB) is a highly selective physical barrier separating blood circulation from the central nervous system. It is formed by tight junctions between brain endothelial cells, which selectively prevent the diffusion of molecules (Cecchelli *et al.*, 2007). Compounds may cross the BBB by two primary pathways: i) paracellular transport, in which compounds pass between the endothelial cells, and ii) transcellular transport via transcytosis thought endothelial cells (Hersh *et al.,* 2016 and Cecchelli *et al.*, 2007). Selective transporters and efflux pumps are expressed by the endothelial cells comprising the BBB, which contribute to the regulating passage of molecules

(Abdelwahed *et al.,* 2008). As a result, the BBB prevents the majority of therapeutic drugs issued by intravenous or oral administration from passing into the brain (Lahiani-Skiba *et al.,* 2006). In particular, larger substances such as vesicles or liposomes are generally unable to penetrate the brain cells (Lundy *et al.*, 2019). However, some promising examples of aforementioned assemblies act as carriers that are able to cross the BBB (Hersh *et al.*, 2016, Vieira and Gamarra, 2016 and Lundy *et al.*, 2019).

In this context, cyclodextrin derivatives (Coisne *et al.*, 2016, Vecsernyés *et al.*, 2014), especially amphiphilic cyclodextrins (CDs) are promising tools to serve as drug delivery systems to the central nervous system (CNS; Bonnet *et al.*, 2015). β-cyclodextrin (β-CD) are cyclic oligosaccharides composed of seven α-(1→4) linked D-glucopyranosides obtained by the enzymatic degradation of starch. They possess a hydrophobic toroidal cavity which is well known to allow the encapsulation of a wide range of hydrophobic molecules. This property is widely exploited to enhance the solubilisation of poorly aqueous soluble drugs (Dodziuk, 2006). Derivatives of CDs could be useful to form supramolecular assemblies such as nanoparticles, and they can also be associated with phospholipid to form mixed vesicles. (Kauscher *et al.*, 2013)

The chemistry of amphiphilic cyclodextrins remains challenging, because it requires either per- or mono-substitution of CD to obtain well-defined structures which are suitable as drug carriers (Sallas and Darcy, 2008). Numerous chemical modifications have been carried out on CDs by grafting alkyl chains of variable length to different positions in order to obtain amphiphilic derivatives. It was previously demonstrated that such derivatives were able to form supramolecular aggregates, which acted as potential drug carriers (Bilensoy *et al.*, 2009). For example, CDs have been modified with hydrophobic moieties (e.g., with cholesteryl, glycerolipidyl or phospholipidyl unit) to target membranes (Auzely-Velty *et al.,* 1999, Moutard *et al.,* 2002 and Furlan *et al.,* 2018). To simplify synthesis, aliphatic chains were also grafted directly onto β-CDs to produce amphiphilic compounds that were able to be incorporated in lipid bilayers (Gallois-Montbrun *et al.,* 2007, Oliva *et al.,* 2020). Nevertheless, in most cases reported in the literature, cyclodextrin-based nanoparticles are only obtained in pure water (Choisnard *et al.,* 2006, McNicholas *et al.,* 2007 and Abdelwahed *et al.,* 2008) or stabilized in biocompatible buffers in the presence of surfactants such as Pluronic PE/F68, Tween 80, Mantonox®80 or Miglyol® 812 (Lahiani-Skiba *et al.,* 2006, Noomen *et al.,* 2008 and Gèze *et al.,* 2009). Several years ago, we designed new amphiphilic permethylated β-CD bearing a phosphoramide moiety which linked a spacer arm and two oleyl chains to the cyclodextrin scaffold. The presence of phosphoramide considerably enhanced the polarity of the entire system, favourising the so-called hydrophilic/hydrophobic balance, which is a desired property for drug delivery in biological media. (Gervaise *et al.*, 2012). The introduction of these two lipid chains was achieved in one step by an Atherton–Todd coupling. These compounds appeared to be very promising for drug delivery with the efficient encapsulation of carboxyfluorescein and scopolamine in several physiological conditions. Nevertheless, the synthesis was not very versatile, and the quantities obtained were not sufficient for further biological studies.

In this work, we investigated the interaction of vesicles, including lipophosphoramidyl permethylated β-CDs (Lip-β-CDs) encapsulating atazanavir (ATV), with the endothelial cells of the BBB. The drug candidate is a well-known protease inhibitor used as an antiretroviral agent against HIV. Nevertheless, the ATV transfer rate through the BBB is very low, resulting in a poor therapeutic effect in cerebrospinal fluid to efficiently protect against HIV replication (Ene *et al.,* 2011,

Varatharajan and Thomas, 2009). In addition to greatly improving the synthesis of a library of Lip-β-CDs, several physico-chemical experiments to delineate the effect of chain length were performed. The results were analysed and discussed in terms of various parameters, such as nanoparticle size and stability, encapsulation capacity, loading efficiency and cellular toxicity and uptake using a human BBB model (Heymans *et al.*, 2018, Jahne *et al.*, 2016 and Hachem *et al.*, 2016).

2. Material and methods

2.1. Material and reagents

β- and γ-cyclodextrins were purchased from Wacker Chemicals (Munich, Germany) whereas β-Alanine methyl ester hydrochloride was from TCI Europe (Zwijndrecht, Belgium). High purity fatty alcohols as most of the reagents were from Sigma- Aldrich (Saint-quentin Fallavier, France). Reyataz capsules, a generous gift from Amiens University Hospital, were treated by liquid liquid extractions to keep pure atazanavir (ATV) only. Fluka supplied solvents (Saint-quentin Fallavier, France). *N,N*-dimethylformamide (DMF) was distilled beforehand under argon atmosphere (on barium oxide) and stored on molecular sieves prior to use. Deuterated solvents were purchased from Eurisotop (Saint-Aubin, France). Atazanavir sulfate, [3H], 1-5 Ci (37-185 GBq)/mmol, were obtained from Hartmann Analytic (Braunschweig, Germany). Sucrose, [14C(U)], 400-700mCi (14.8-25.9GBq)/mmol were supplied from PerkinElmer (Les Ulis, France).

Details of used devices for thin layer chromatography (TLC), Chromatography, mass spectrometry (MS), nuclear magnetic resonance (NMR), Dynamic light scattering (DLS) and Fluorimetry are available in SI.

2.2. Synthesis Procedures

Oleylphosphites **1-4** were already described in literature (Mevel *et al.*, 2007 and 2008). Characterization were in accordance with data in literature as well as 6^{VI}-amino-6^{VI}-deoxy-2^{II},3^{III}-di-*O*-methyl-hexakis(2,3,6-tri-*O*-methyl)cyclomaltoheptaose **13** (Gervaise *et al.,* 2012). Description of the synthesis of compounds **5-12** is available in SI.

6^{VI}-amido-β-alanyl-(6^{VI}-di(dodecyloxy)phosphoramidyl)-6^{VI}-deoxy-2^{II},3^{III}-di-*O*-methyl-hexakis(2,3,6-tri-*O*-methyl)-cyclomaltoheptaose 15

O,O-didodecyl-*N*-(2-carboxyethyl)phosphoramidate **9** (268 mg, 0.53 mmol, 1.5 eq) was dissolved in anhydrous *N*,*N* dimethylformamide (20 mL) under argon. Then, 1-hydroxybenzotriazole (472 mg, 3.5 mmol, 10 eq) and *N*,*N*-diisopropylcarbodiimide (545 µL, 3.5 mmol, 10 eq) were added. After stirring for 2h, the 6^{VI}-amino-6^{VI}-deoxy-2^{II},3^{III}-di-*O*-methyl-hexakis(2,3,6-tri-*O*-methyl)cyclomaltoheptaose **13** solution (495 mg, 0.35 mmol, 1 eq dissolved in 20 mL of chloroform with few drops of triethylamine) was added. The reaction mixture was stirred at room temperature for 24h. The solvent was removed by evaporation under reduced pressure and the residue was purified by column chromatography on silica gel DCM/MeOH (98/2 and 95/5) with 71% yield. TLC: Rf = 0.51 (DCM/MeOH 95:5 (v/v)) ^{1}H NMR (300 MHz, $CDCl_3$), δ (ppm): 6.18 (m, 1H, NH), 5.13 (m, 7H, H_1, H^{I}), 3.94 (m, 4H, $H_{1'}$), 3.90-3.29 (m, 35H, H_3, H^{III}, H_4, H^{IV}, H_5, H^{V}, H_6, H^{VI}) , 3.62 (s, 18H, $O_{(6)}CH_3$), 3.50 (s, 21H, $O_{(3)}CH_3$), 3.37 (s, 21H, $O_{(2)}CH_3$), 3.19 (m, 9H, H_2, H^{II}, H_9), 2.37 (t, 2H, H_8),1.62 (m, 4H, $H_{2'}$) , 1.25 (m, 36H, $H_{3'}$-$H_{11'}$), 0.87 (t, 6H, $H_{12'}$, $J_{H12'\text{-}H11'}$= 6.49 Hz) ^{13}C NMR (75 MHz, $CDCl_3$), δ (ppm): 99.20 (7C, C_1, C^{I}), 82.20-80.79 (21C, C_2, C^{II}, C_3, C^{III}, C_4, C^{IV}), 71.38, 71.19 (13C, C_6, C_5, C^{V}), 66.67 (2C, $C_{1'}$), 61.61 (6C, $O_{(6)}CH_3$), 59.16-58.76 (7C, $O_{(3)}CH_3$, $O_{(2)}CH_3$), 39.97 (1C, C^{VI}), 37.95 (2C, C_8, C_9), 32.05-22.82 (20C, $C_{2'}$-$C_{11'}$), 14.24 (2C, $C_{12'}$) ^{31}P NMR (120 MHz,

$CDCl_3$), δ (ppm): 110.46 (s, 1P) HRMS (ESI): m/z 973.5291 $[M+2Na]^{2+}$, ($C_{89}H_{165}N_2O_{38}PNa_2$ requires 973.5281, m/z 1924.0685 $[M+Na]^+$, ($C_{89}H_{165}N_2O_{38}PNa$ requires 1924.0670).

6^{VI}-amido-β-alanyl-(6^{VI}-di(tetradecyloxy)phosphoramidyl)-6^{VI}-deoxy-2^{II},3^{III}-di-*O*-methyl-hexakis(2,3,6-tri-*O*-methyl)-cyclomaltoheptaose 16

O,O-ditetradecyl-*N*-(2-carboxyethyl)phosphoramidate **10** (174 mg, 0.48 mmol, 2.3 eq) was dissolved in anhydrous *N*,*N* dimethylformamide (6.7 mL) and methylene chloride (25 mL) under argon. Then, 1-hydroxybenzotriazole (430 mg, 3.182 mmol, 15 eq) and *N*,*N*-diisopropylcarbodiimide (500 µL, 0.318 mmol, 15 eq) were added. After stirring for 3h, the 6^{VI}-amino-6^{V}I-deoxy-2^{II},3^{III}-di-*O*-methyl-hexakis(2,3,6-tri-*O*-methyl)cyclomaltoheptaose **13** solution (300 mg, 0.212 mmol, 1 eq dissolved in 2.5 mL of methylene chloride with few drops of triethylamine) was added. The reaction mixture was stirred at room temperature for 24h. The solvent was removed by evaporation under reduced pressure and the residue was purified by column chromatography on silica gel DCM/MeOH (100/0, 95/5 and 8/2) with 68% yield. TLC Rf = 0.44 (DCM/MeOH 95:5 (v/v)) ^{1}H NMR (300 MHz, $CDCl_3$) δ (ppm): 6.20 (s, 1H, NH), 5.16-5.07 (m, 7H, H_1, H^{I}), 3.95 (t, 4H, $H_{1'}$), 3.97-3.45 (m, 35H, H_3, H^{III}, H_4, H^{IV}, H_5, H^{V}, H_6, H^{VI}), 3.63 (s, 18H, $O_{(6)}CH_3$), 3.50 (s, 21H, $O_{(3)}CH_3$), 3.38 (s, 21H, $O_{(2)}CH_3$), 3.24 (m, 9H, H_2, H^{II}, H_9), 2.35 (t, 2H, H_8), 1.62 (m, 4H, $H_{2'}$), 1,24 (m, 44H, $H_{3'\text{-}13'}$), 0,86 (t, 6H, $H_{14'}$, $J_{H14'\text{-}H13'}$= 6.35 Hz); ^{13}C NMR (75 MHz, $CDCl_3$), δ (ppm): 99.16 (7C, C_1, C^{I}), 81.94-80.44 (21C, C_2, C^{II}, C_3, C^{III}, C_4, C^{IV}), 71.35 (14C, C_5, C^{V}, C_6, C^{VI}), 66.65 (2C, $C^{1'}$), 61.57 (6C, $O_{(6)}CH_3$), 59.12 (7C, $O_{(2)}CH_3$), 58.43 (7C, $O_{(3)}CH_3$), 37.90 (2C, C_8, C_9), 32.57-22.80 (24C, $C_{2'\text{-}13'}$), 14.22 (2C, $C_{14'}$) ^{31}P NMR (120 MHz, $CDCl_3$), δ (ppm): 110,51 (s, 1P) and HRMS (ESI): m/z 1001.5603 $[M+2Na]^{2+}$, ($C_{93}H_{173}N_2O_{38}PNa_2$ requires 1001.5594).

6^{VI}-amido-β-alanyl-(6^{VI}-di(hexadecyloxy)phosphoramidyl)-6^{VI}-deoxy-2^{II},3^{III}-di-*O*-methyl-hexakis(2,3,6-tri-*O*-methyl)-cyclomaltoheptaose 17

O,O-dihexadecyl-*N*-(2-carboxyethyl)phosphoramidate **11** (288 mg, 0.467 mmol, 1,5 eq) was dissolved in anhydrous *N*,*N* dimethylformamide (10 mL) and methylene chloride (40 mL) under argon. Then, 1-hydroxybenzotriazole (420 mg, 3.11 mmol, 10 eq) and *N*,*N*-diisopropylcarbodiimide (720 µL, 4.61 mmol, 15 eq) were added. After stirring for 3h, the 6^{VI}-amino-6^{VI}-deoxy-2^{II},3^{III}-di-*O*-methyl-hexakis(2,3,6-tri-*O*-methyl)cyclomaltoheptaose **13** solution (440 mg, 0.31 mmol, 1 eq dissolved in 4 mL of methylene chloride with few drops of triethylamine) was added. The reaction mixture was stirred at room temperature for 24h. The solvent was removed by evaporation under reduced pressure and the residue was dissolved in methylene chloride and cooled at -20°C. 1-hydroxybenzotriazole was precipitated and removed by filtration. Then, the residue was purified by column chromatography on silica gel DCM/MeOH (100/0, 95/5 and 8/2) with 78% yield. TLC: Rf = 0.44 (DCM/MeOH 95:5 (v/v)) ^{1}H NMR (300 MHz, $CDCl_3$), δ (ppm): 6.15 (m, 1H, NH), 5.11 (m, 7H, H_1, H^{I}), 3.90 (m, 4H, $H_{1'}$), 3.80-3.45 (m, 35H, H_3, H^{III}, H_4, H^{IV}, H_5, H^{V}, H_6, H^{VI}) , 3.63 (s, 18H, $O_{(6)}CH_3$), 3.50 (s, 21H, $O_{(3)}CH_3$), 3.38 (s, 21H, $O_{(2)}CH_3$), 3.14 (m, 9H, H_2, H^{II}, H_9), 2.31 (t, 2H, H_8),1.54 (m, 4H, $H_{2'}$) , 1.17 (m, 52H, $H_{3'}$-$H_{15'}$), 0.81 (t, 6H, $H_{16'}$, $J_{H16'\text{-}H15'}$= 6.39 Hz) ^{13}C NMR (75 MHz, $CDCl_3$), δ (ppm): 99.03 (7C, C_1, C^{I}), 81.81-80.30 (21C, C_2, C^{II}, C_3, C^{III}, C_4, C^{IV}), 70.92 (14C, C_5, C^{V}, C_6, C^{VI}), 66.52 (2C, $C_{1'}$), 61.44 (6C, $O_{(6)}CH_3$), 59.00-58.47 (14C, $O_{(3)}CH_3$, $O_{(2)}CH_3$), 37.81 (2C, C_8, C_9), 31.89-22.66 (28C, $C_{2'}$-$C_{15'}$), 14.09 (2C, $C_{16'}$) ^{31}P NMR (120 MHz, $CDCl_3$), δ (ppm): 110.53 (s, 1P) and HRMS (ESI): m/z 2036.1959 $[M+Na]^+$, ($C_{97}H_{181}N_2O_{38}PNa$ requires 2036.1928).

6^{VI}-amido-β-alanyl-(6^{VI}-di(oleyloxy)phosphoramidyl)-6^{VI}-deoxy-2^{II},3^{III}-di-*O*-methyl-hexakis(2,3,6-tri-*O*-methyl)-cyclomaltoheptaose 18

O,O-dioleyl-*N*-(2-carboxyethyl)phosphoramidate **12** (283 mg, 0.42 mmol, 1.5 eq) was dissolved in anhydrous *N*,*N* dimethylformamide (15 mL) under argon. Then, 1-hydroxybenzotriazole (378 mg, 2.8 mmol, 10 eq) and *N*,*N*-diisopropylcarbodiimide (436 µL, 2.8 mmol, 10 eq) were added. After stirring for 1h, the 6^{VI}-amino-6^{VI}-deoxy-2^{II},3^{III}-di-*O*-methyl-hexakis(2,3,6-tri-*O*-methyl)cyclomaltoheptaose **13** solution (395 mg, 0.28 mmol, 1 eq dissolved in 10 mL of chloroform with few drops of triethylamine) was added. The reaction mixture was stirred at room temperature for 24h. The solvent was removed by evaporation under reduced pressure and the residue was dissolved in methylene chloride and cooled at -20°C. 1-hydroxybenzotriazole was precipated and removed by filtration. Then, the residue was purified by column chromatography on silica gel DCM/MeOH (98/2 and 96/4) with 85% yield. TLC: Rf = 0.42 (DCM/MeOH 95:5 (v/v)) ^{1}H NMR (300 MHz, $CDCl_3$), δ (ppm): 6.17 (m, 1H, NH), 5.33 (m, 4H, $H_{9'}$, $H_{10'}$), 5.12 (m, 7H, H_1, H^I), 3.96 (m, 4H, $H_{1'}$), 3.89-3.41 (m, 35H, H_3, H^{III}, H_4, H^{IV}, H_5, H^V, H_6, H^{VI}) , 3.62 (s, 18H, $O_{(6)}CH_3$), 3.50 (s, 21H, $O_{(3)}CH_3$), 3.37 (s, 21H, $O_{(2)}CH_3$), 3.17 (m, 9H, H_2, H^{II}, H_9), 2.36 (t, 2H, H_8), 1.99 (m, 8H, $H_{8'}$, $H_{11'}$), 1.64 (m, 4H, $H_{2'}$) , 1.26 (m, 44H, $H_{3'\text{-}7'}$, $H_{12'\text{-}17'}$), 0.87 (t, 6H, $H_{18'}$, $J_{H18'\text{-}H17'}$ = 6.37 Hz) ^{13}C NMR (75 MHz, $CDCl_3$), δ (ppm): 130.13 (4C, $C_{9'}$, $C_{10'}$), 99.20 (7C, C_1, C^I), 82.21-80.47 (21C, C_2, C^{II}, C_3, C^{III}, C_4, C^{IV}), 71.38-71.08 (13C, C_5, C^V, C_6), 66.65 (2C, $C_{1'}$), 61.61 (6C, $O_{(6)}CH_3$), 59.16-58.49 (14C, $O_{(3)}CH_3$, $O_{(2)}CH_3$), 39.96 (1C, C^{VI}), 37.94 (2C, C_8, C_9), 32.75-22.82 (28C, $C_{2'}$-$C_{8'}$, $C_{11'}$-$C_{17'}$), 14.25 (2C, $C_{18'}$) ^{31}P NMR (120 MHz, $CDCl_3$), δ (ppm): 110.55 (s, 1P) HRMS (ESI): m/z 1055.6066 $[M+2Na]^{2+}$, ($C_{101}H_{185}N_2O_{38}PNa_2$ requires 1055.6064).

6^{VI}-mono-amino-6^{VI}-deoxy-2^{II},3^{III}-di-*O*-methyl-heptakis(2,3,6-tri-*O*-methyl) cyclomaltooctaose 14

γ-CD (5.0 g, 3.85 mmol, 1 eq) was solubilized in pyridine (300 mL) under argon. After the solubilization (40 min), the 2,4,6-triisopropyl sulfonyl chloride (3.5 g, 11.56 mmol, 3 eq) was added. The reaction mixture has been stirred at room temperature under argon for 24h. Then, the solvent was removed by evaporation under reduced pressure until there is a minimum of solvent and acetone (500 mL) was added. The precipitation obtained was filtered and was washed with acetone. The white powder of 6^{VI}-(O-2,4,6-triisopropylbenzenesulfonyl)-cyclomaltooctaose was put in desiccator at 60°C under reduced pressure one night.

Then, the 6^{VI}-(O-2,4,6-triisopropylbenzenesulfonyl)-cyclomaltooctaose (6.07 g, 3.89 mmol, 1 eq) was dissolved in DMF (130 mL) at 80°C. After solubilization, the sodium azide (0.51 g, 7.77 mmol, 2 eq) was added and the reaction mixture has been stirred at 80°C for 24h. Then, the solvent was removed by evaporation under reduced pressure, a little bit of water has been added to solubilize the product and acetone (200 mL) was added. The precipitation obtained was filtered and was washed with acetone. The white powder of 6^{VI}-azido-6^{VI}-deoxy-cyclomaltooctaose was put in desiccator at 60°C under reduced pressure one night.

Then, the 6^{VI}-azido-6^{VI}-deoxy-cyclomaltooctaose (1.72 g, 1.30 mmol, 1 eq) was dissolved in dry DMF (70 mL). The solution was cooled down at 0°C in ice bath and sodium hydride (60%, m/m) (3.12 g, 78.1 mmol, 60 eq) was added. After solubilization, methyl iodide (15 mL, 240.9 mmol, 185 eq) was added. The reaction mixture has been stirred at room temperature and under inert atmosphere for 1 day. The addition of few drops of ethanol stopped the reaction. The reaction mixture is then filtered and the filtrate was evaporated under reduced pressure. The obtained oil was put in a minimum of water and extracted with dichloromethane (3x50 mL). The organic phase was washed with water (2x50 mL), dried on sodium sulfate, filtered and the solvent was removed by evaporation under reduced pressure. A yellow oil was obtained which is a mixture of the expected compound and the

per(2,3,6-tri-*O*-methyl)cyclomaltooctaose, formed from the γ-CD regenerated during the synthesis of 6^{VI}-azido-6^{VI}-deoxy-cyclomaltooctaose. This mixture would be purified in the next step.

Then, the 6^{VI}-mono-azido-6^{VI}-deoxy-2^{II},3^{III}-di-O-methyl-heptakis(2,3,6-tri-O-methyl) cyclomaltooctaose (3.041 g, 1.85 mmol, 1 eq) was dissolved in DMF (155 mL). After solubilization, the triphenyl phosphine (2.43 g, 9.25 mmol, 5 eq) was added and the reaction mixture has been stirred at room temperature for 2h. The solution was cooled down at 0°C in ice bath and ammoniac solution (85 mL, 38%) was added drop by drop. The reaction mixture has been stirred at room temperature for 1 night. Then, the residue was purified by column chromatography on silica gel DCM/MeOH (100/0, 95/5 and 8/2) with 5% global yield. TLC: Rf = 0.52 (DCM/MeOH 9/1 (v/v)) ^{1}H NMR (300MHz, $CDCl_3$), δ (ppm): 5.21 (m, 8H, H1, H^I), 3.91-3.30 (m, 49H, H_2, H_{II}, H_3, H_{III}, H_4, H_{IV}, H_5, H_V, H_6, H_{VI}), 3.64 (s, 21H, $O_{(6)}CH_3$), 3.51 (s, 24H, $O_{(3)}CH_3$), 3.37 (s, 24H, $O_{(2)}CH_3$), 3.21 (m, 8H, H_2, H^{II}). ^{13}C NMR (75MHz, $CDCl_3$), δ (ppm): 98.05 (8C, C1, C^I), 82.00 (24C, C_2, C^{II}, C_3, C^{III}, C_4, C^{IV}), 71.30 (7C, C6), 70.92 (8C, C_5, C^V), 61.43 (8C, $O_{(6)}CH_3$), 59.18 (7C, $O_{(3)}CH_3$), 58.88 (7C, $O_{(2)}CH_3$). ZQ (ESI): m/z 1641.0 $[M+Na]^+$ ($C_{71}H_{127}NO_{39}Na$ requires 1640.80)

6^{VI}-amido-β-alanyl-(6^{VI}-di(dodecyloxy)phosphoramidyl)-6^{VI}-deoxy-2^{II},3^{III}-di-*O*-methyl-heptakis(2,3,6-tri-*O*-methyl)-cyclomaltooctaose 19

O,O-didodecyl-*N*-(2-carboxyethyl)phosphoramidate (51 mg, 0.10 mmol, 1.5 eq) was dissolved in anhydrous *N*,*N* dimethylformamide (3 mL) under argon. Then, 1-hydroxybenzotriazole (90 mg, 0.67 mmol, 10 eq) and *N*,*N*-diisopropylcarbodiimide (100 µL, 0.67 mmol, 10 eq) were added. After stirring for 2h, the 6^{VI}-amino-6^{VI}-deoxy-2^{II},3^{III}-di-*O*-methyl-heptakis(2,3,6-tri-*O*-methyl)cyclomaltooctaose solution (108 mg, 0.067 mmol, 1 eq dissolved in 3 mL of chloroform with few drops of triethylamine) was added. The reaction mixture was stirred at room temperature for 24h. The solvent was removed by evaporation under reduced pressure and the residue was purified by column chromatography on silica gel DCM/MeOH (98/2 and 95/5) with 52%. TLC: Rf = 0.46 (DCM/MeOH 9/1 (v/v)) ^{1}H NMR (300 MHz, $CDCl_3$), δ (ppm): 6.18 (m, 1H, NH), 5.13 (m, 8H, H_1, H^I), 3.94 (m, 4H, $H_{1'}$), 3.90-3.29 (m, 35H, H_3, H^{III}, H_4, H^{IV}, H_5, H^V, H_6, H^{VI}) , 3.62 (s, 18H, $O_{(6)}CH_3$), 3.50 (s, 21H, $O_{(3)}CH_3$), 3.37 (s, 21H, $O_{(2)}CH_3$), 3.19 (m, 10H, H_2, H^{II}, H_9), 2.37 (t, 2H, H_8),1.62 (m, 4H, $H_{2'}$) , 1.25 (m, 36H, $H_{3'}$-$H_{11'}$), 0.87 (t, 6H, $H_{12'}$, $J_{H12'H11'}$ = 6.41 Hz) ^{13}C NMR (75 MHz, $CDCl_3$), δ (ppm): 99.20 (8C, C_1, C^I), 82.20-80.79 (24C, C_2, C^{II}, C_3, C^{III}, C_4, C^{IV}), 71.38, 71.19 (15C, C_6, C_5, C^V), 66.67 (2C, $C_{1'}$), 61.61 (7C, $O_{(6)}CH_3$), 59.16-58.76 (16C, $O_{(3)}CH_3$, $O_{(2)}CH_3$), 39.97 (1C, C^{VI}), 37.95 (2C, C_8, C_9), 32.05-22.82 (20C, $C_{2'}$-$C_{11'}$), 14.24 (2C, $C_{12'}$) ^{31}P NMR (120 MHz, $CDCl_3$), δ (ppm): 110.46 (s, 1P) ZQ (ESI): m/z 2129.9 $[M+Na]^+$ ($C_{98}H_{181}N_2O_{43}PNa$ requires 2128.18)

6^{VI}-amido-β-alanyl-(6^{VI}-di(tetradecyloxy)phosphoramidyl)-6^{VI}-deoxy-2^{II},3^{III}-di-*O*-methyl-heptakis(2,3,6-tri-*O*-methyl)-cyclomaltooctaose 20

O,O-ditetradecyl-*N*-(2-carboxyethyl)phosphoramidate (52mg, 0.093mmol, 1.5eq) was dissolved in anhydrous *N*,*N* dimethylformamide (3mL) under argon. Then, 1-hydroxybenzotriazole (83mg, 0.62mmol, 10eq) and *N*,*N*-diisopropylcarbodiimide (96µL, 0.62mmol, 10eq) were added. After stirring for 2h, the 6VI-amino-6VI-deoxy-2II,3III-di-*O*-methyl-heptakis(2,3,6-tri-*O*-methyl)cyclomaltooctaose solution (100mg, 0.062mmol, 1eq dissolved in 3mL of methylene chloride with few drops of triethylamine) was added. The reaction mixture was stirred at room temperature for 24h. The solvent was removed by evaporation under reduced pressure and the residue was purified by column chromatography on silica gel DCM/MeOH (98/2 and 95/5) with 54%.^{1}H NMR (300

MHz, $CDCl_3$), δ (ppm): 6.16 (m, 1H, NH), 5.26 (m, 8H, H_1, H^I), 3.94 (m, 4H, $H_{1'}$), 3.87-3.37 (m, 35H, H_3, H^{III}, H_4, H^{IV}, H_5, H^V, H_6, H^{VI}) , 3.63 (s, 18H, $O_{(6)}CH_3$), 3.51 (s, 21H, $O_{(3)}CH_3$), 3.37 (s, 21H, $O_{(2)}CH_3$), 3.19 (m, 9H, H_2, H^{II}, H_9), 2.37 (m, 2H, H_8),1.64 (m, 4H, $H_{2'}$), 1.25 (m, 48H, $H_{3'}$-$H_{13'}$), 0.87 (t, 6H, $H_{12'}$, $J_{H14'-H13'}$ = 6.41 Hz) ^{13}C NMR (75 MHz, $CDCl_3$), δ (ppm): 98.07 (8C, C_1, C^I), 82.14 (24C, C_2, C^{II}, C_3, C^{III}, C_4, C^{IV}), 71.33, 70.93(15C, C_6, C_5, C^V), 66.69 (2C, $C_{1'}$), 61.36 (7C, $O_{(6)}CH_3$), 59.17 (16C, $O_{(3)}CH_3$, $O_{(2)}CH_3$), 40.00 (1C, C^{VI}), 37.91 (2C, C_8, C_9), 32.06-22.84 (24C, $C_{2'}$-$C_{13'}$), 14.28 (2C, $C_{12'}$) ZQ (ESI): m/z 2185.3 $[M+Na]^+$ ($C_{102}H_{189}N_2O_{43}PNa$ requires 2184.24)

2.3. Vesicles preparation and characterization

The nanoparticle preparation used is the lipidic film rehydration. Our compounds solubilized in ethanol and the 1-Palmitoyl-2-oleoylphosphatidylcholine (POPC) solubilized in hexane/ethanol (9:1 v/v) were mixed, with or without ATV (20µL of 5mM in EtOH). Then, the organic solvent was evaporated by nitrogen flux and the dry film was placed in desiccator for 2h to remove any trace of organic solvent. Then, the dry film is rehydrated by 2mL of Ringer-Hepes (RH) buffer pH 7.4 to reach a final concentration of 400 µM. The dry film was re-suspended by vigorous homogenization to produce MLVs. Then the solution is sonicated for 3 cycles at 2 min 30s (power: 33% of 500 W, probe diameter: 13 mm, Bioblock Scientific VibraCellTM 75115) followed by a filtration on 0.2 µm filters (Tuffryn® by Acrodisc®) to eliminate titanium particles from the probe. The excess of ATV which was not encapsulated in the vesicles is eliminated by Size Exclusion Chromatography (SEC, Sephadex G50, length: 5 cm, diameter: 1.5 cm). The loaded vesicles are collected in the tubes 3 and 4, corresponding to an elution volume of ≈3 and ≈4 mL, respectively. In the case of ^3H-ATV, concentration was measured after SEC at 0.975 µM using Liquid Scintillation Analyser.

2.4. Calibration curve of Atazanavir fluorescence intensity in Ringer-Hepes buffer pH 7.4

This calibration curve was performed with a fluorescence spectrometer Synergy H1 (BioTek, Winooski, USA). A stock solution of ATV in DMSO (10 mM) is prepared. This compound is not soluble directly in the RH buffer, so, first, 5 µL of the ATV stock solution was putted in a small pillbox and then the RH was added (2 mL) to reach the concentration of 25 µM. An optimization of the measurement is performed to have the better S/N ratio in the RH. It is found that the better emission and excitation wavelengths are λ_{ex} = 290 nm and λ_{em} = 338 nm, respectively.
Then, from the stock solution (25 µM) a cascade dilution by 2 is performed and the fluorescence measurements were performed. The limit of detection is determined at 0.4 µM and the calibration curve obtained (see Figure S1).

2.5. Atazanavir *in vitro* drug release

100 µL of CD/POPC mixed vesicle and POPC vesicle charged with ATV in RH buffer pH 7.4, prepared following the procedure described above, were dialyzed using Single-Use Rapid Equilibrium Dialysis (Thermo Scientific™). NPs were placed in vertical cylinder of dialysis membrane with a molecular-weight cutoff of 8 kDa. 300 µL of RH buffer pH 7.4 were placed in buffer chamber. The plate with dialysis membranes was placed at 37°C under vigorous shaking. ATV was quantified in both drug and buffer chambers by fluorescence spectroscopy.

2.6. *In vitro* model of blood brain barrier

Bovine Brain Capillary Endothelial Cells (BBCECs) were cultivated during 12 days with rat glial cell in Transwell™ Costar polycarbonate inserts, 3 µm pore size, coated with rat tail collagen. The resulting co-culture was maintained for at least 12 days under standard conditions: a humidified 5% CO_2 atmosphere, with renewal of the culture medium (DMEM supplemented with 10% Horse Serum, 10% Calf Serum, 1% glutamine and 0.5% gentamycin) every second days. Under these conditions, BBCECs exhibit most of the characteristics of the BBB such as low permeability to non-permanent markers (Schultz *et al.,* 2015, Candela *et al.,* 2008, Dehouck *et al.,* 1992 and Culot *et al.,* 2008).
All experiments were performed in triplicate and at 37°C. On the day of the experiment, β-CDs were dissolved at the selected concentration in HEPES- buffered Ringer´s solution (NaCl 150 mM, KCl 5.2 mM, $CaCl_2$ 2.2 mM, $MgCl_2$ 0.2 mM, $NaHCO_3$ 6 mM, Glucose 2.8 mM, HEPES 5 mM, water for injection). At the start of the transport experiments, buffered 2.5 mL of Ringer´s solution was added to the receiver compartments without cells. Inserts with bovine brain endothelial cells were then placed in these wells and 1.5 mL compound's solution were added to the donor compartment.

Endothelial permeability coefficients (Pe) were calculated as described previously (Dehouck, 1992). In this calculation, both filter without cell permeability (PSf = filter with collagen coating) and filter with cell permeability (PSt = filter with collagen with ECs) were taken into account.
Pe = 1/PSe = 1/PSt + 1/PSf, where PS denote for the permeability over the surface area (in mL/min) which was the slope determined by linear regression of the average volume of compound cleared (Cl) versus time over the experiment. PSf was the collagen coated filter permeability previously determined. PSt was calculated using the volume of compound cleared (Cl in mL or cm^3) at each time interval following the equation:
Cl = A / Cd. Where, A was the amount of compound in the basolateral compartment (in mol), Cd was the concentration in the luminal compartment (in mol/cm^3). The total cleared volume at each time point was calculated by summing Cl at each time interval. EC permeability coefficient (Pe, cm/min) was obtained by dividing PSe values by the surface area of the filter (cm^2), as follow: Pe = PSe / S.
Toxicity study of tested compounds was performed using radiolabelled sucrose (^{14}C sucrose) which is a paracellular marker to control the toxicity of products. This small hydrophilic molecule presents, in physiological conditions, a low cerebral penetration and its endothelial permeability coefficient reveals the endothelial cell monolayer integrity.
The co-incubation of ^{14}C sucrose (final concentration 1.82KBq/mL) with the tested compound was performed in triplicates. Co-incubation of ^{14}C sucrose and the tested compound allows to assess drug toxicity by evaluating the permeability coefficient for ^{14}C sucrose. ^{14}C-sucrose was analyzed using Liquid Scintillation Analyser (Tri-carb 2100TR).

2.7. Uptake of ^{3}H-Atazanavir in endothelial cells

After 120 minutes of drug transport experiment, inserts ± BBCECs were washed 5 times with cold RH buffer pH 7.4. Cells were lysed with 500 µL of the triton X100 1% solution. Cell lysates and Filters were transferred to polyethylene scintillation vials with addition of scintillation cocktail (Ultima Gold MW). The amounts of ^{3}H-ATV were determined using Liquid Scintillation Analyser (Tri-carb 2100TR).

2.8. Preparation of POPC/ fluorescent probe (R18) vesicles

40 µL POPC solubilized in hexane/ethanol (9/1 v/v) mixture (5 mM) was put in a pillbox. The R18 probe is introduced at 6.3 mass% compared the mass of lipid, so 9.58 µL (1 mg/mL in ethanol) was

added to the POPC in the pillbox. Then, the same procedure is applied as for the formation of the NPs

2.9. Fusogenicity studies

To study fusogenicity, the fluorescence measurements were performed with a Cary Elipse fluorescence spectrometer using a quartz cell. The final concentration, in the cell, is fixed at 50 µM with a 1:4 molar ratio between the vesicles of amphiphilic CD/POPC and R18/POPC. So, a volume of 100 µL of each vesicle is added. Kinetics measurements were performed during 31 min. First, 800 µL of TRIS buffer pH 7.4 with 100 µL of R18/POPC was mixed and the measurement was performed during 1 min to obtain the value of "zero fusion". Then, the CD/POPC is added and the measurement is performed.

3. Results and discussion

3.1. Synthesis of lipophosphoramidyl permethylated CDs

An optimisation of the synthesis of Lip-β-CDs **15–18** was performed in order to scale up the synthesis which was previously described (Gervaise *et al.*, 2012). Fatty alcohols reacted with diphenylphosphite in a Kugelrohr apparatus, leading quantitatively to dialkylphosphite **1–4**, depending on the chain length i.e. C12, C14 to C16 and C18:1 according to elsewhere described procedure (Mevel *et al.*, 2007 and 2008). Fatty phosphites **1–4** are then introduced in Todd-Atherton reaction with β-alanine methyl ester with rather good yield (Figure 1 and see SI for experimental details). After the saponification of methyl ester to **9–12** (see SI for experimental details), a peptidic coupling with permethylated 6-amino-6-deoxy-β-cyclodextrin **14** obtained by the conventional route (Gervaise *et al.*, 2012) was performed. Five compounds were obtained in the gram scale with good yields (65–85%). The second advantage of this new process is the versatility of the synthesis in terms of tuning oligosaccharidic macrocycle or aliphatic chains.

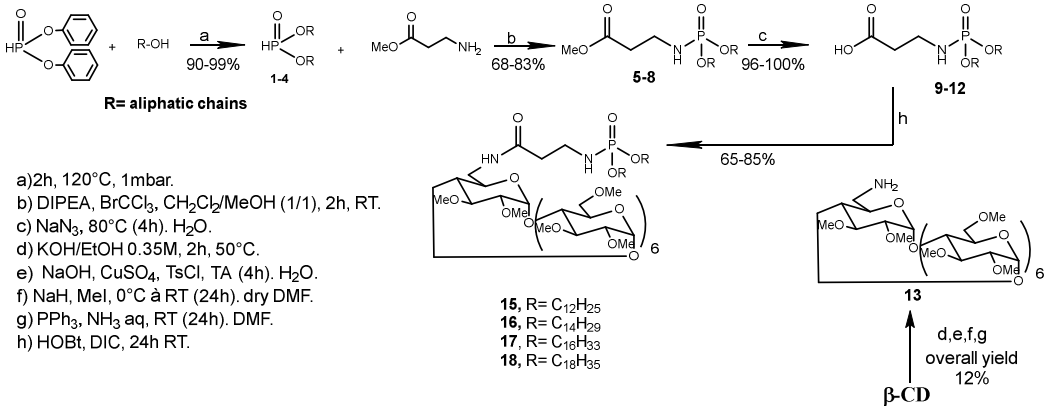

Figure 1: Chemical convergent route to lipophosphoramidyl-β-CDs **15–18**.

We demonstrated that this route could also be applied to permethylated 6-amino-6-deoxy-γ-cyclodextrin with C12 **19** and C14 **20** chain lengths (Figure 2) obtained with 52% and 54%, respectively (for the scheme of the chemical route see Figure S2). The difficulty is the preparation of the permethylated 6-amino-6-deoxy-γ-CD **14**, which was obtained only at a 5% yield. The first monomodification step of γ-CD was performed using triisopropylsulfonyl chloride, as described in the literature (Palin *et al.*, 2001). The yield of this step was very low, impairing the scale-up of these compounds for further experiments.

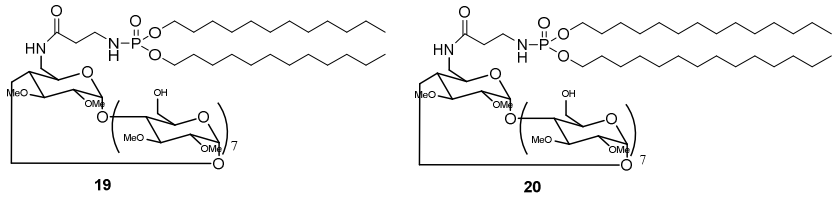

19 **20**

Figure 2: Lipophosphoramidyl-γ-CD **19** and **20** obtained by the same pathway.

3.2. Characterization of Lipophosphoramidyl permethylated β-CDs

Our goal is to achieve an *in vitro* test, in which a high purity of the compounds is a mandatory condition. We thus performed a very thorough characterization of the structure of our compounds by NMR (Figure 3 for **15** and see Figures S3–S8 for other compounds) and used mass spectrometry to decipher the structural backbone.

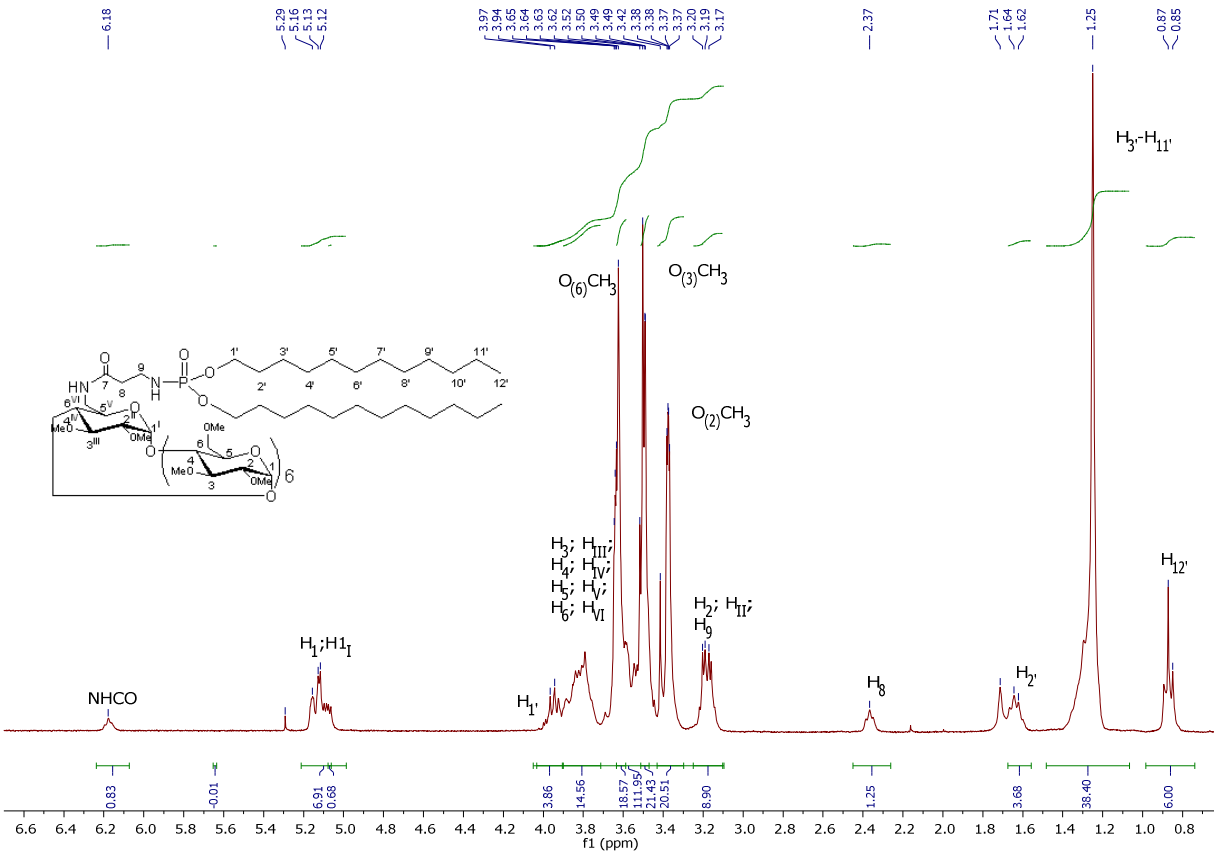

Figure 3: ^{1}H NMR of lipophosphoramidyl permethylated β-CD C12 **15** in $CDCl_3$ (298K, 400 MHz)

The ^{1}H NMR spectrum of compound **15** shows a high resolution in a nonpolar solvent, meaning that the pure mono-substituted compound and NH of the amide group at δ = 6.18 ppm is characteristic of the linkage of the carboxylic acid of lipidic part to the amino group of the cyclodextrin.

Full MS spectra showed that ions were only detected under 1+ and 2+ charge states with common H^+, NH_4^+, Na^+ and K^+ cations. Whatever the compounds, sodiated forms are the prominent ions, singly and doubly charged, for compounds **15** (Figure 4), **16** and **18** (Figure S9 and S10).

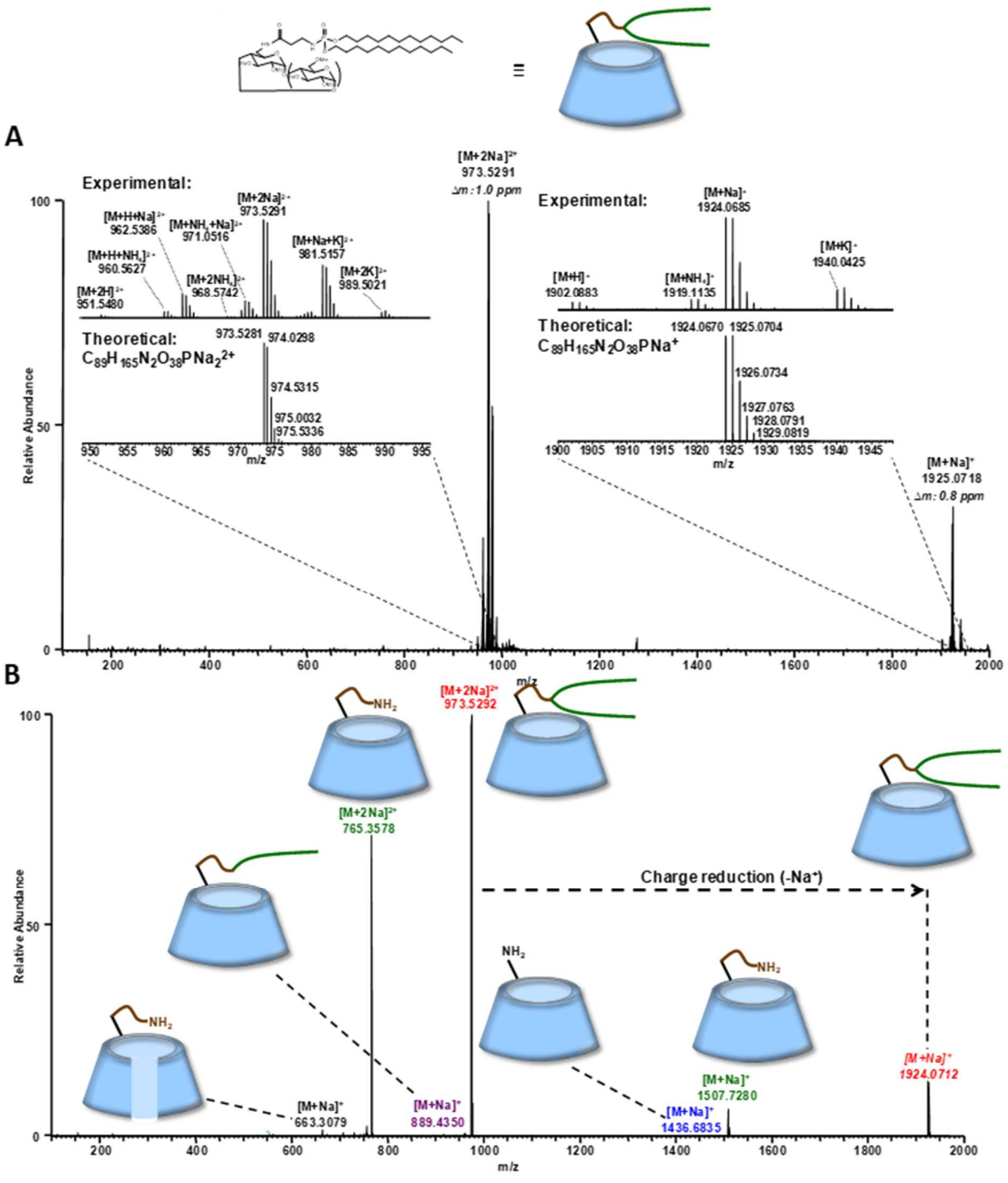

Figure 4. ESI-HRMS and ESI-HRMS/MS of compound **15**. A) Full MS spectrum and B) MS/MS spectrum obtained for fragmentation of $[M+2Na]^{2+}$ in HCD at 40% (73eV). The two insets show the comparison between experimental and theoretical m/z for singly and doubly sodiated species.

Exact masses were also confirmed by ESI-HRMS, for example, for $[M+2Na]^{2+}$ with experimental m/z 973.5291 (theoretical 973.5281; Δm: 1.0 ppm), 1001.5603 (theoretical 1001.5594; Δm: 0.9 ppm) and 1055.6066 (theoretical 1055.6062; Δm: 0.2 ppm) for compounds **15**, **16** and **18**, respectively. For **17**, ESI-HRMS measured m/z 2036.1959 for $[M+Na]^+$ (theoretical 2036.1928; Δm: 1.5 ppm). Moreover, even if MS is not a quantitative approach, clear spectra with no noticeable impurities were obtained.
Plotting the precursor abundance according to the HCD deposited energy allowed the well-known survival yield curves to be accessed and the CE_{50} values, that is, the energy required to decompose 50% of the initial precursor, to be obtained (Przybylski *et al.*, 2015). Moreover, as previously highlighted, the energy employed during HCD fragmentation can be directly provided in an eV scale. These values can be used to compare the stability of various molecular structures within a family of similar compounds. Here, deducted CE_{50} values were equal to 40.3 (73eV), 40.4 (76eV) and 40.1% (79eV) for doubly sodiated species of compounds **15**, **16** and **18** respectively (see Figure S11). Comparison of CE_{50} values reveals that the gradual increase of acyl chains length leads to a slight strengthening of the molecular stability, that is, from 73 to 79 eV for C12 to C18:1, respectively. Careful examination of the MS/MS spectrum of the doubly sodiated ion of compound **15** obtained at its CE_{50} value (40%) may portray the main decomposition products, highlighting the most exposed moiety (Figure 4B). Hence, in addition to a usual charge reduction (the loss of one Na^+) at m/z 1924.0712, various fragments can be observed. The most intense fragment at m/z 765.3578 corresponds to the cleavage of the phosphoramide bond (N-P), leading to the release of a whole phosphoramidyl group. Such loss was confirmed by the same remaining 6-amido-β-alanyl-6-deoxy-TRIMEB as a monosodiated form at m/z 1507.7280. At least three other ions were also easily detected at m/z 1436.68, m/z 889.4350 and m/z 663.3079. The former corresponds to mono-amino-TRIMEB and the latter to a 6-amido-β–alanyl-6-deoxy-TRIMEB which has lost one methylated glucose (MeGlc). The third ion, at m/z 889.4350, is particularly interesting, since it indicates that one full chain remains between the two. Such results can be tentatively explained by a self-inclusion phenomenon (i.e., the insertion of one of **15**'s own lipid chains inside β-CD hydrophobic cavity), as previously observed by us and others especially for dioleoyl-glycerolipidyl-β-CD (Furlan *et al.*, 2018). Indeed, such self-inclusion of one lipid chain can partially prevent this chain from undergoing a fragmentation process.

To both track fragmentation trends and map the genealogies of product ions originating from consecutive losses, an energy-resolved mass spectrometry (ERMS) strategy was undertaken on compound **15**. ERMS was, in particular, successfully used to characterize structural isomers of oligosaccharides (Kurimoto *et al.*, 2006), to capture glycan connectivity in glycopeptides (Kolli and Dodds, 2014) and to delineate Lipid A variants (Crittenden *et al.*, 2017).

As an example, we investigated ERMS in an MS/MS energy–variable manner to characterize structural features, via dominant fragmentation pathways, corresponding to the doubly sodiated species of compound **15** (Figure S12).

As already described, from the low range of this HCD deposited (< 30%, < 55 eV), only one fragment appears to correspond to 6-amido-β-alanyl-6-deoxy-TRIMEB, starting from 23% (41 eV; Figure S12 A, full dark green trace). As the collision energy was increased from 30% (55 eV), the precursor ion was progressively and constantly fragmented, leading to the apparition of mono-amino-TRIMEB (Figure S12B, full blue trace) and compound **15** with one lipidyl chain lost (Figure S12C, violet trace). This last

result is quite surprising, since amido-β-alanyl-6-deoxy-TRIMEB was logically expected to be the main fragment of a consecutive fragmentation of lipophosphoramidyl moieties. Nonetheless, such results can be assumed by a parallel fragmentation pathway originating from a different conformation of compound **15**. Such an alternative supports the aforementioned hypothesis as regards a self-inclusion phenomenon and demonstrates the co-existence of two populations of compounds, that is, a first one with two free pending lipidic chains and a second conformation involving one fatty acid chain included in the cavity of the CD. Moreover, the use of collision-induced dissociation (CID) in place of HCD allowed for operation at a slower energy regime but with a higher number of collisions, leading to the formation of monolipidyl-phosphoramidyl-MeGlc (Figure S13). Fragmentation pathways were proposed according to these results in Figure S14. All these structural deciphering experiments showed that compounds were present both in high purity grade and with well-defined structures and thus could be confidently used for biological assessment.

The toxicity of these compounds was then tested on an *in vitro* model of the BBB. This model aimed to co-cultivate bovine brain capillary endothelial cells from rat glial cells. This model has been intensively characterized and is widely used to test drug toxicity. This parameter is checked by measuring the permeability of a small hydrophilic compound, the ^{14}C sucrose, across the cell monolayer. As shown by Figure 5, the labelled sucrose passage across the BBCEC monolayer was not altered in presence of concentrations below 5 µM of amphiphilic CDs (Figure 5). The permeability below $0.75.10^{-3}$ cm.min^{-1} at 5µM for **15–17**, which is lower than that of β-CD(C9)$_2$OOMe, another amphiphilic cyclodextrin tested previously (Oliva *et al*. 2020). At 50 µM, **15** increased ^{14}C Sucrose permeability, suggesting that the lowest concentrations must be used for further studies.

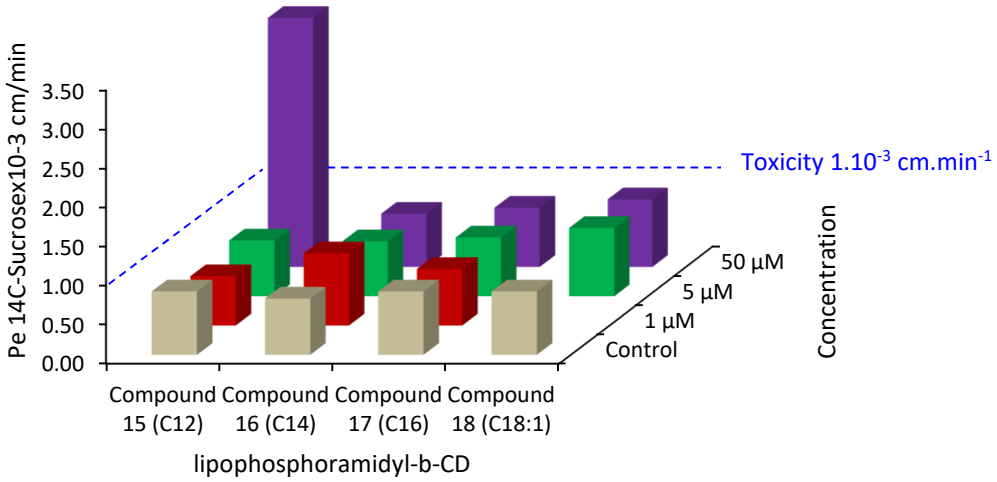

Figure 5: Study of the permeability of ^{14}C sucrose on an *in vitro* BBB model in the presence of various amphiphilic cyclodextrins **15** (C12), **16** (C14), **17** (C16) and **18** (C18:1).

The choice of mixed vesicles seems to be a good strategy to form vesicles both reducing the quantity of the amphiphilic CDs needed and preventing toxicity against the BBB (Binkowski-Machut, 2006 and Vieira et Gamarra, 2016).

3.3. Preparation of vesicles containing Atazanavir

Our goal is to prepare mixed vesicles composed of phospholipid (POPC) and three amphiphilic cyclodextrins of the family and encapsulating ATV. To control the size of the vesicles, the film hydration technique was chosen to formulate the Lip-β-CDs with POPC in presence of the drug. The diameter of the mixed vesicles prepared with ATV was measured by DLS to be in the range 150–210 nm depending on the aliphatic chain. The polydispersity index (PdI) for **15**/POPC is low, involving monodisperse vesicles, whereas Lip-β-CDs with longer chains exhibit a higher PdI, revealing quite polydisperse particles (Table 1). The size of these vesicles is consistent with an application for transcytose on the blood brain barrier. Recently, Lundy *et al*. (Lundy *et al.*, 2019) highlighted that a size in the 50–200 nm range is generally accepted as optimal.

Table 1: Measurements by DLS of the diameter of vesicles obtained for three formulations varying by chain length of lipidic moiety (n = 3).

Vesicles formulation	Diameter (nm)	PdI
15(C12)/POPC/ATV	171	0.192
16(C14)/POPC/ATV	210	0.296
18(C18 :1)/POPC/ATV	149	0.302

Our vesicles could be assimilated to niosomes. Indeed, in the literature, nano-niosomes were described as vesicles composed of cholesteryl derivatives and non-ionic surfactants, especially glycolipidic ones (Moghassemi and Hadjizadeh, 2014). They can be prepared by the film hydration technique. Niosomes with β-CD have already been successfully employed to improve cellular uptake of drugs (Oommen *et al.* 1999).

We studied the *in vitro* release of ATV from POPC liposomes or mixed vesicles of amphiphilic cyclodextrins/POPC compared to ATV alone (Figure 6). Atazanavir is poorly soluble in an aqueous buffer, so we work in diluted conditions. Moreover, the formulations led to colloidal stable suspension.

In four hours, 100% of ATV alone was released, whereas in the case of mixed vesicles, 40–50% of the ATV was released in approximately two hours. The same profile was observed regardless of the amphiphilic CD in the formulation (data not shown). However, during the same duration, we observed an ATV release of 80% with the liposomes of POPC alone. In this case, the curve obtained is close to that of ATV alone. We thus demonstrated the efficiency of amphiphilic CD in slowly releasing a drug such as ATV. This result is in good agreement with the encapsulation and release of methotrexate using noisome-based CDs (Oommen *et al* 1999).

After seven days, the release of ATV was not complete with amphiphilic CD/POPC vesicles. This could be due to a lack of detection sensitivity, because of chemical degradation of ATV. Indeed, ATV is known to be unstable in aqueous solutions and rather sensitive to heat and slightly basic conditions (Dey *et al.* 2017).

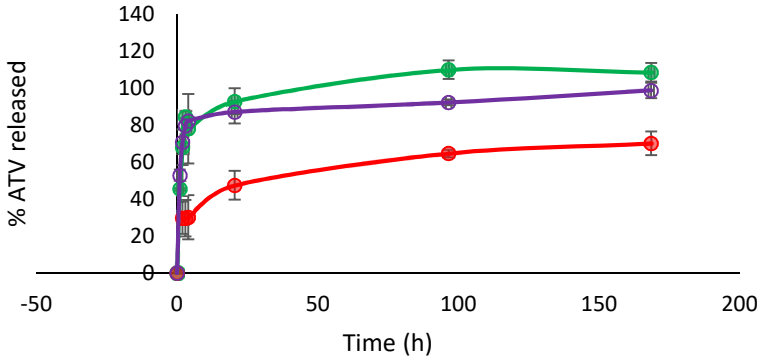

Figure 6: *In vitro* release of ATV encapsulated in mixed vesicles of POPC/amphiphilic CD **15** (red●), POPC liposome (violet ■) compared to ATV alone (green ▲)

3.4. *In vitro* BBB model toxicity and transport experiments

We then checked the toxicity of vesicles alone on the BBB cells by measuring the permeability of the barrier in contact with different concentrations of vesicles (0 – 400 µM). At concentrations below 50 µM of vesicles, no alteration of the permeability inferior to 0.8. 10^{-3} cm/min of the monolayer was observed, much less than quaternary ammonium βCD (QAβCD) nanoparticles already used as carriers on the BBB model with no toxicity (Gil *et al*. 2009).

Knowing that the integrity of the model was demonstrated, further experiments were carried out to improve the transport of ^{3}H-ATV through the BBB *in vitro* model. It was not technically possible to detect ^{3}H-ATV in the abluminal side of the model, but we showed a significant enhancement (Figure 7) of the cellular uptake of ^{3}H-ATV in the endothelial cells of the BBB. Mixed vesicles composed of **18**/POPC were thus able to enhance the intracellular accumulation of ^{3}H-ATV by four-fold or higher, showing a clear endocytosis of vesicles by endothelial cells. Mixed vesicles containing amphiphilic CDs with shorter chains, **15** and **16**, are less efficient as drug carriers but also enhanced uptake, by 1.1 and 1.6 fold, respectively. This result is consistent with features of efficient drug carriers reported in the literature. Comparatively, doxorubicin uptake in the BBB model was enhanced by 2.2 fold with QAβCD nanoparticles (Gil *et al*. 2009), whereas the concentration of ribavirin, included in niosomes, was six-fold higher in liver cells than free drug (Hashim *et al*. 2010).

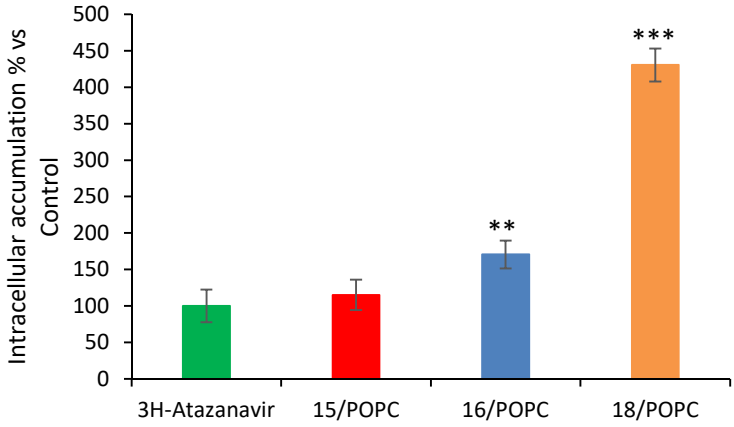

Figure 7: Cellular accumulation of ^{3}H-ATV formulated in mixed vesicles amphiphilic CD **15**, **16** and **18,** respectively, with POPC (Normalization with respect to the internalization of ^{3}H-ATV alone in endothelial cells).**p < 0.01, ***p < 0.001.

The rationalisation of this clear impact of the chain length on cellular uptake requires a good understanding of the effect of Lip-β-CDs **15**, **16** and **18**/POPC vesicles on a membrane model. The fusogenicity of various vesicles was thus evaluated by fluorescence measurements. Two different vesicles were prepared, one with various molar ratio of Lip-β-CDs /POPC one using R18 as a fluorescent probe and three phosphatidylcholines (POPC:PLPC:SAPC (1:1:1)), sphingomyelin, cholesterol 4:3:1 as a biomimetic model of the plasmic membrane. One minute after mixing both of these vesicles, an increase of fluorescence was noted leading to larger vesicle formation involving dequenching of fluorescence due to fusogenic properties (Figure 8). These results indicate that a very strong fusogenicity of **15**/POPC with a 20–50% molar ratio occurred, in contrast to when POPC alone is used as a control. A maximum fluorescence rate was reached around 70%, portraying good fusion with biomimetic SUVs. The behaviour of **15**/POPC mixed vesicles is very similar to that described by Kros *et al*., who used lipopeptides incorporated in liposomes to produce the fusion of lipid membranes (Marsden *et al*. 2013). Conversely, compound **16**–based mixed vesicles exhibited a maximum fluorescence rate at approximatively 35% with biomimetic SUVs. That shows a less fusogenic character with the biomimetic membrane than **15**. As regards **18**/POPC mixed vesicles, we still observed a low fusogenicity, which is close to that obtained with POPC SUVs alone. Because of the fusogenicity, vesicles are probably diluted in the membranes of cells before acting as carriers through membrane cells and consequently preventing the endocytosis process.

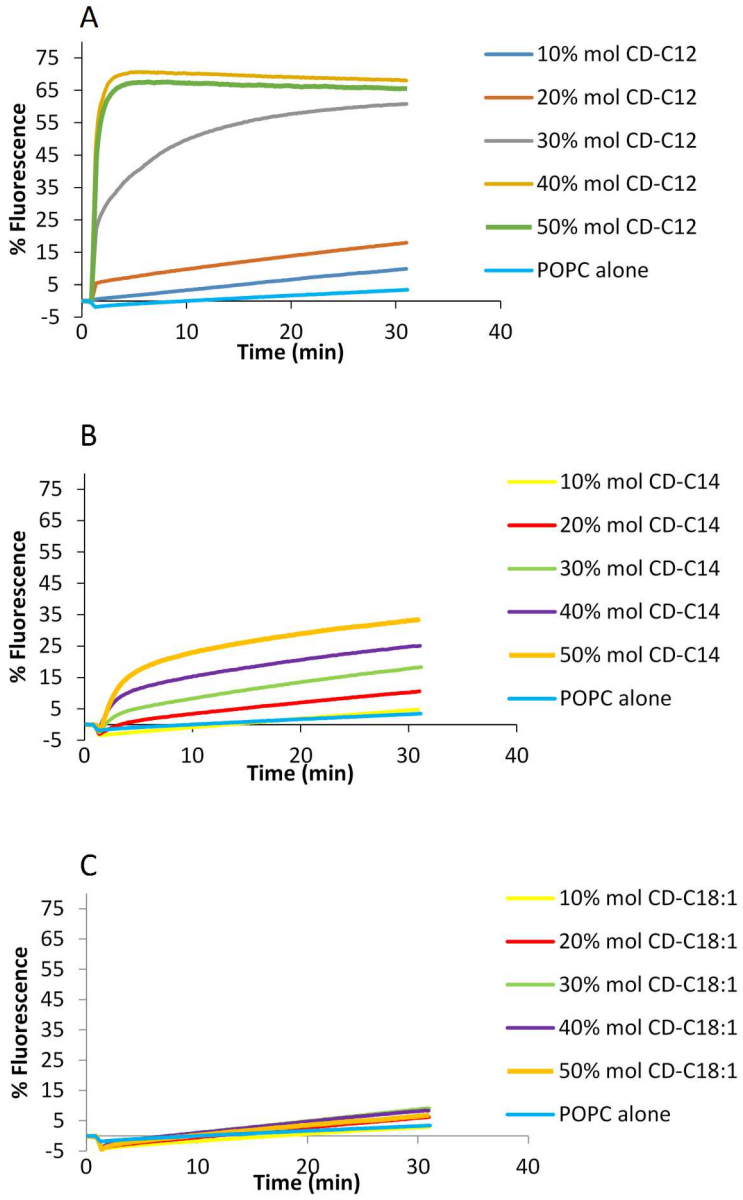

Figure 8: Fusogenicity effect of lipophosphoramidyl β-CDs/POPC mixed vesicles on R18/4:3:1 phosphatidylcholines (POPC :PLPC : SAPC (1:1:1)), sphingomyelin, cholesterol vesicles in a TRIS buffer (10 mM, NaCl 150 mM, pH 7,4). **15** (A), **16** (B) and **18** (C).

4. Conclusion

In this study, we proposed an efficient synthetic route to prepare lipophosphoramidyl CDs at the gram scale. Obtained amounts of each compound were able to be assembled in vesicles with POPC encapsulating antiretroviral drugs, that is, ATV. Conversely to usual liposomes, a slow and controlled release was observed thanks to lipophosphoramidyl CDs vesicles. Moreover, two particularly important features were highlighted: (i) the absence of toxicity observed on an *in vitro* BBB model as a critical aspect for drug delivery applications and (ii) a high enhancement of cellular uptake of ATV in endothelial cells for oleylphosphoramidyl CDs (C18:1, compound **18**). This clear impact of chain

length can be explained by fusogenicity properties regarding the grafted chain length. Indeed, oleylphosphoramidyl CDs exhibit a very low fusogenicity, which prevents the dilution of vesicles in the membrane and presumably increases the drug delivery rate into the cell.

Acknowledgments
This work and the PhD grant (FN) was supported, as part of the "Agroressources" Research Program, by the Conseil Régional de Picardie under the name SYNVECT.

References
Abdelwahed, W., Degobert, G., Dubes, A., Parrot-Lopez, H., Fessi, H. (2008) Sulfated and non-sulfated amphiphilic β-cyclodextrins: Impact of their structural properties on the physicochemical properties of nanoparticles. Int. J. Pharm., 351, 289-295, https://doi.org/10.1016/j.ijpharm.2007.09.035.

Auzely-Velty, R., Perly, B., Tache, O., Zemb, T., Jehan, P., Guenot, P., Dalbiez, J.P., Djedaini-Pilard, F. (1999). Cholesteryl-cyclodextrins: synthesis and insertion into phospholipid membranes, Carbohydr. Res., 318, 82-90, https://doi.org/10.1016/S0008-6215(99)00086-5.

Azad, T. D., Pan, J., Connolly, I. D., Remington, A., Wilson, C. M., Grant, G. A. (2015) Therapeutic Strategies to Improve Drug Delivery across the Blood-Brain Barrier. Neurosurg. Focus, 38, E9, https://doi.org/10.3171/2014.12.FOCUS14758

Binkowski-Machut, C., Hapiot, F., Martin, P., Cecchelli, R., Monflier, E. (2006) How cyclodextrins can mask their toxic effect on the blood–brain barrier. Bioorg. Med. Chem. Lett., 16, 1784–1787, https://doi.org/10.1016/j.bmcl.2006.01.031

Bilensoy, E., Hincal, A.A. (2009) Recent advances and future directions in amphiphilic cyclodextrin nanoparticles, Expert Opin. Drug Delivery, 6 1161-1173, https://doi.org/10.1517/17425240903222218

Bonnet, V., Gervaise, C., Djedaïni-Pilard, F., Furlan, A., Sarazin, C. (2015) Cyclodextrin nanoassemblies: a promising tool for drug delivery, Drug Discovery Today, 20(9), 1120-1126, https://doi.org/10.1016/j.drudis.2015.05.008.

Candela, P., Gosselet, F., Miller, F., Buee-Scherrer, V., Torpier, G., Cecchelli, R., Fenart, L. (2008) Physiological pathway for low-density lipoproteins across the blood-brain barrier: transcytosis through brain capillary endothelial cells in vitro. Endothelium. 5(5-6), 254-264, doi: 10.1080/10623320802487759.

Cecchelli, R., Berezowski, V., Lundquist, S., Maxime Culot, Renftel, M., Dehouck M-P. Fenart L. (2007) Modelling of the blood–brain barrier in drug discovery and development. Nat. Rev. Drug. Discov., 6, 650–661, https://doi.org/10.1038/nrd2368

Choisnard, L., Gèze, A., Putaux, J.L., Wong, Y.S., Wouessidjewe, D. (2006) Nanoparticles of β-cyclodextrin esters obtained by self-assembling of biotransesterified β-cyclodextrins. Biomacromolecules, 7, 515-520, https://doi.org/10.1021/bm0507655.

Coisne, C., Tilloy, S., Monflier, E., Wils, D., Fenart, L., Gosselet, F. (2016) Cyclodextrins as Emerging Therapeutic Tools in the Treatment of Cholesterol-Associated Vascular and Neurodegenerative Diseases. Molecules, 21, 1748, https://doi.org/10.3390/molecules21121748.

Crittenden, C.M., Akin, L.D., Morrison, L.J., Trent, M.S., Brodbelt, J.S. (2017). Characterization of Lipid A Variants by Energy-Resolved Mass Spectrometry: Impact of Acyl Chains. J. Am. Soc. Mass Spectrom., 28(6), 1118–1126. https://doi.org/10.1007/s13361-016-1542-6

Culot, M., Lundquist, S., Vanuxeem, D., Nion, S., Landry, C., Delplace, Y., Dehouck, M.P., Berezowski, V., Fenart, L., Cecchelli, R. (2008) An in vitro blood-brain barrier model for high throughput (HTS) toxicological screening., Toxicol. In Vitro., 22(3), 799-811, doi: 10.1016/j.tiv.2007.12.016.

Dehouck, M.P., Jolliet-Riant, P., Brée, F., Fruchart, J.C., Cecchelli, R., Tillement, J.P. (1992). Drug transfer across the blood-brain barrier: correlation between in vitro and in vivo models. J. Neurochem., 58(5), 1790-1797, https://doi.org/10.1111/j.1471-4159.1992.tb10055.x.

Dey, S., Subhasis Patro S., Suresh Babu, N., Murthy, P.N., Panda, S.K. (2017). Development and validation of a stability-indicating RP–HPLC method for estimation of atazanavir sulfate in bulk. J. Pharm. Anal., 7, 134-140.

Dodziuk, H., (2006) Cyclodextrins and Their Complexes. Chemistry, Analytical Methods, Applications; Ed.; Wiley-VCH: New York, ISBN: 978-3-527-60844-7.

Ene, L., Duiculescu, D., Ruta, S.M. (2011) How much do antiretroviral drugs penetrate into the central nervous system?. *J Med Life*. 4(4), 432–439.

Furlan, A.L., Buchoux, S., Miao, Y., Banchet, V., Létévé, M., Lambertyn, V., Michel, J., Sarazin, C., Bonnet, V. (2018) Nanoparticles based on lipidyl-β-cyclodextrins: synthesis, characterization, and experimental and computational biophysical studies for encapsulation of atazanavir. New J. Chem., 42, 20171-20179, https://doi.org/10.1039/C8NJ03237H.

Gallois-Montbrun, D., Thiebault, N., Moreau, V., Lebas, G., Archambault, J.-C., Lesieur, S., Djedaıni-Pilard, F. (2007) Direct synthesis of novel amphiphilic cyclodextrins, J. Incl. Phenom. Macrocylic. Chem., 57, 131-135, https://doi.org/10.1007/s10847-006-9208-9.

Gervaise, C., Bonnet, V., Wattraint, O., Aubry, F., Sarazin, C., Jaffrès, P-A., Djedaïni-Pilard, F. (2012) Synthesis of lipophosphoramidyl-cyclodextrins and their supramolecular properties. Biochimie, 94 (1)66-74, https://doi.org/10.1016/j.biochi.2011.09.005.

Gèze, A., Choisnard, L., Putaux, J.L., Wouessidjewe, D. (2009) Colloidal systems made of biotransfered α, β and γ cyclodextrins grafted with C10 alkyls chains. Mat. Sci. Eng. C, 29, 458-462, https://doi.org/10.1016/j.msec.2008.08.027.

Gil, E.S., Li, J., Xiao, H., Lowe, T.L. (2009) Quaternary Ammonium β-Cyclodextrin Nanoparticles for Enhancing Doxorubicin Permeability across the In Vitro Blood-Brain Barrier. Biomacromol., 10, 505–516, https://doi.org/10.1021/bm801026k.

Hachem, M., Géloën, A., Van, A.L., Foumaux, B., Fenart, L., Gosselet, F., Da Silva, P., Breton, G., Lagarde, M., Picq, M., Bernoud-Hubac, N. (2016). Efficient Docosahexaenoic Acid Uptake by the Brain from a Structured Phospholipid. Mol. Neurobiol., 53(5), 3205-3215, doi: 10.1007/s12035-015-9228-9.

Hashim, F., El-Ridy, M., Nasr, M., Abdallah, Y. (2010) Preparation and characterization of niosomes containing ribavirin for liver targeting, Drug Delivery, 17:5, 282-287, DOI: 10.3109/10717541003706257

Hersh, D.S., Wadajkar, A.S., Roberts, N., Perez, J.G., Connolly, N.P., Frenkel, V., Winkles, J.A., Woodworth, G.F., Kim, A.J. (2016) Evolving Drug Delivery Strategies to Overcome the Blood Brain Barrier. Curr Pharm Des., 22(9), 1177–1193, https://doi.org/10.2174/1381612822666151221150733

Heymans, M., Sevin, E., Gosselet, F., Lundquist, S., Culot, M. (2018). Mimicking brain tissue binding in an in vitro model of the blood-brain barrier illustrates differences between in vitro and in vivo methods for assessing the rate of brain penetration. Eur. J. Pharm. Biopharm., 127, 453-461, https://doi.org/10.1016/j.ejpb.2018.03.007.

Jähne, E.A., Eigenmann, D.E., Sampath, C., Butterweck, V., Culot, M., Cecchelli, R., Gosselet, F., Walter F.R., Deli M.A., Smieško, M., Hamburger, M., Oufir, M. (2016) Pharmacokinetics and In Vitro Blood-Brain Barrier Screening of the Plant-Derived Alkaloid Tryptanthrin. Planta Med., 82(11-12), 1021-1029. doi: 10.1055/s-0042-105295.

Kauscher, U., Stuart, M.C.A., Drücker, P., Galla, H-J., Ravoo, B.J. (2013) Incorporation of Amphiphilic Cyclodextrins into Liposomes as Artificial Receptor Units, Langmuir, 29, 7377-7383, https://doi.org/10.1021/la3045434.

Kolli, V., Dodds, E.D. (2014). Energy-resolved collision-induced dissociation pathways of model N-linked glycopeptides: implications for capturing glycan connectivity and peptide sequence in a single experiment. Analyst, 139(9), 2144-2153, doi:10.1039/C3AN02342G.

Kurimoto, A., Daikoku, S., Mutsuga, S., Kanie, O. (2006). Analysis of Energy-Resolved Mass Spectra at MSn in a Pursuit To Characterize Structural Isomers of Oligosaccharides. Anal. Chem., 78(10), 3461-3466, https://doi.org/10.1021/ac0601361

Lahiani-Skiba, M., Bounoure, F., Shawky-Tous, S., Arnaud, P., Skiba, M. (2006) Optimization of entrapment of metronidazole in amphiphilic β-cylodextrin nanospheres. J. Pharm. Biomed. Anal., 41, 1017-1021, https://doi.org/10.1016/j.jpba.2006.01.021 .

Lundy, D.J., Lee, K-J., Peng, I-C., Hsu, C-H., Lin, J-H., Chen, K-H., Tien, Y-W., Hsieh, P.C.H. (2019). Inducing a Transient Increase in Blood−Brain Barrier Permeability for Improved Liposomal Drug Therapy of Glioblastoma Multiforme, ACS Nano*, 13* (1), 97-113, DOI: 10.1021/acsnano.8b03785

Marsden, H.R., Korobko, A.V., Zheng, T. Voskuhl, J., Kros, A. (2013) Controlled liposome fusion mediated by SNARE protein mimics. Biomater. Sci., 2013, 1, 1046-1054, 10.1039/c3bm60040h.

McNicholas, S., Rencurosi, A., Lay, L., Mazzaglia, A., Sturiale, L., Perez, M., Darcy, R. (2007) Amphiphilic *N*-glycosyl-thiocarbamoyl cyclodextrins: Synthesis, self-assembly, and fluorimetry of recognition by *lens culinaris* lectin. Biomacromolecules, 8, 1851-1857, https://doi.org/10.1021/bm070055u.

Mével, M., Montier, T., Lamarche, F., Delépine, P., Le Gall, T., Yaouanc, J.J., Jaffrès, P.A., Cartier, D., Lehn, P., Clément, J.C. (2007) Dicationic lipophosphoramidates as DNA carriers, Bioconjugate Chem., 18, 1604-1611, https://doi.org/10.1021/bc070089z .

Mével, M., Neveu, C., Gonçalves, C., Yaouanc, J.J., Pichon, C., Jaffrès, P.A., Midoux, P. (2008) Novel neutral imidazole-lipophosphoramides for transfection assays, Chem. Commun. 3124-3126, http://dx.doi.org/10.1039/B805226C.

Moghassemi, S., Hadjizadeh, A., (2014) Nano-niosomes as nanoscale drug delivery systems: An illustrated review, J. Control. Release, 185, 22-36, 10.1016/j.jconrel.2014.04.015

Moutard, S., Perly, B., Godé, P., Demailly, G., Djedaïni-Pilard, F. (2002) Novel glycolipids based on cyclodextrins, J. Incl. Phenom. Macrocylic. Chem., 44, 317-322, 10.1023/A:1023014718447.

Neuwelt, E., Bauer, B., Fahlke, C., Fricker, G., Iadecola, C., Janigro, D., Leybaert, L., Molnar, Z., O'Donnell, M. E., Povlishock, J. T., Saunders, N. R., Sharp, F., Stanimirovic, D., Watts, R. J., Drewes, L. R. (2011). Engaging Neuroscience to Advance Translational Research in Brain Barrier Biology. Nat. Rev. Neurosci., 12, 169−182, 10.1038/nrn2995

Noomen, A., Hbaieb, S., Parrot-Lopez, H., Kalfat, R., Fessi, H., Amdouni, N., Chevalier, Y. (2008) Emulsions of β-cyclodextrins grafted to silicone for the transport of antifungal drugs. Mat. Sci. Eng. C, 28, 705-715, 10.1016/j.msec.2007.10.057.

Oliva, E., Mathiron, D., Rigaud, S., Monflier, E., Sevin, E., Bricout, H., Tilloy, S., Gosselet, F., Fenart, L., Bonnet, V., Pilard, S., Djedaini-Pilard, F. (2020). New Lipidyl-Cyclodextrins Obtained by Ring Opening of Methyl Oleate Epoxide Using Ball Milling. Biomolecules*,* 10, 339-356, 10.3390/biom10020339.

Oommen, E., Tiwari, S.B., Udupa, N., Kamath, R., Devi, P.U. (1999). Niosome Entrapped β-Cyclodextrin Methotrexate Complex as a Drug Delivery System. Indian J. Pharmacol., 31, 279-284.

Palin, R., Grove, S.J.A., Brosser, A.B., Zhang, M-Q. (2001). Mono-6-(O-2,4,6-triisopropylbenzenesulfonyl)-γ-cyclodextrin, a novel intermediate for the synthesis of mono-functionalised γ-cyclodextrins. Tetrahedron Letters, 42(50), 8897-8899, 10.1016/S0040-4039(01)01934-7

Przybylski, C. and Bonnet, V. (2013), Discrimination of cyclic and linear oligosaccharides by tandem mass spectrometry using collision-induced dissociation (CID), pulsed-Q-dissociation (PQD) and the higher-energy C-trap dissociation modes. Rapid Commun. Mass Spectrom., 27: 75-87. doi:10.1002/rcm.6422

Przybylski, C., Bonnet, V., Cézard, C. (2015) Probing the common alkali metal affinity of native and variously methylated β-cyclodextrins by combining electrospray-tandem mass spectrometry and molecular modeling. Phys. Chem. Chem. Phys., 17(29), 19288-19305, doi :10.1039/C5CP02895G.

Przybylski, C., Benito, J.M., Bonnet, V., Ortiz Mellet, C., García Fernández, J.M. (2016). Deciphering of polycationic carbohydrate based non-viral gene delivery agents by ESI-LTQ-Orbitrap using CID/HCD pairwise tandem mass spectrometry. RSC Adv., 6(82), 78803-78817, doi :10.1039/C6RA14508F.

Sallas, F., Darcy, R. (2008) Advances in synthesis and supramolecular chemistry, Eur.J.Org.Chem., 957-969, 10.1002/ejoc.200700933.

Schultz, L., Zurich, M.G., Culot, M., da Costa, A., Landry, C., Bellwon, P., Kristl, T., Hörmann, K., Ruzek, S., Aiche, S., Reinert, K., Bielow, C., Gosselet, F., Cecchelli, R., Huber, C.G., Schroeder, O.H., Gramowski-Voss, A., Weiss, D.G., Bal-Price, A. (2015). Evaluation of drug-induced neurotoxicity based on metabolomics, proteomics and electrical activity measurements in complementary CNS in vitro models. Toxicol. In Vitro. 30, 138-165, doi: 10.1016/j.tiv.2015.05.016.

Varatharajana, L., Thomas S.A. (2009). The transport of anti-HIV drugs across blood–CNS interfaces: Summary of current knowledge and recommendations for further research. Antiviral Research, 82 A99–A109, 10.1016/j.antiviral.2008.12.013

Vecsernyés, M., Fenyvesi, F., Bácskay, I., Deli, M.A., Szente, L., Fenyvesi, E. (2014). Cyclodextrins, Blood–Brain Barrier, and Treatment of Neurological Diseases, Archives of Medical Research, 45(8), 711-729, https://doi.org/10.1016/j.arcmed.2014.11.020

Vieira, D.B. and Gamarra, L.F. (2016) Getting into the brain: liposome-based strategies for effective drug delivery across the blood–brain barrier. Int. J. Nanomedicine, 11, 5381–5414, https://doi.org/10.2147/IJN.S117210

Graphical abstract

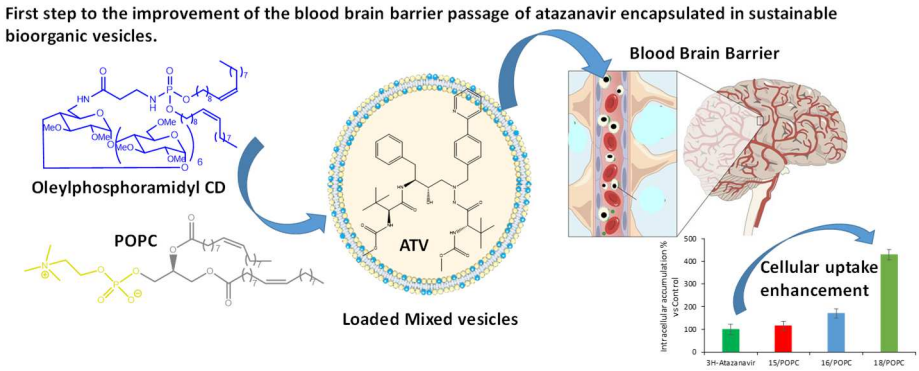

Highlights

- Lipophosphoramidyl cyclodextrins (Lip-β-CDs) were successfully synthesized.
- Controlled release of drug was shown with vesicles POPC/(Lip-β-CDs).
- No toxicity was observed on an *in vitro* BBB model.
- Oleylphosphoramidyl CDs enhanced cellular uptake of Atazanavir in BBB cells.
- The very low fusogenicity of oleylphosphoramidyl Lip-β-CDs increased the drug delivery rate.